Stretching Instability of Helical Springs

David A. Kessler and Yitzhak Rabin
Department of Physics, Bar-Ilan University, Ramat-Gan, Israel
(Received 29 May 2002; published 16 January 2003)

We show that when a gradually increasing tensile force is applied to the ends of a helical spring with sufficiently large ratios of radius to pitch and twist to bending rigidity, the end-to-end distance undergoes a sequence of discontinuous stretching transitions. Subsequent decrease of the force leads to steplike contraction, and hysteresis is observed. For finite helices, the number of these transitions increases with the number of helical turns but only one stretching and one contraction instability survive in the limit of an infinite helix. We calculate the critical line that separates the region of parameters in which the deformation is continuous from that in which stretching instabilities occur.

DOI: 10.1103/PhysRevLett.90.024301 PACS numbers: 46.32.+x, 46.25.Cc, 62.20.Fe

The mechanical instability of systems under external forces is an important phenomenon, the study of which dates back to the solution of the buckling of a thin elastic beam under compression and torque by Euler and his contemporaries [1,2]. The geometry of the system clearly plays an important role in this process. The present paper presents a theoretical prediction of a hitherto unknown instability that arises when a helical spring is stretched by a tensile force applied to its ends. This instability is especially interesting as a result of the current experimental interest in the elastic properties of microscopic objects, ranging from self-assembled helical ribbons in solidifying cholesterol [3] to chromatin [4] to DNA [5]. As we will show in the following, stretching instabilities occur only in helices whose radius is sufficiently larger than their pitch and whose rigidity with respect to twist exceeds that with respect to bending.

Consider a helical spring of contour length L, characterized by its radius r and pitch p (see Fig. 1). For our purposes, it is more convenient to describe the helix in terms of its intrinsic geometrical quantities, the curvature κ, and torsion τ:

$$\kappa = \frac{r}{r^2 + (\frac{p}{2\pi})^2}, \qquad \tau = \frac{\frac{p}{2\pi}}{r^2 + (\frac{p}{2\pi})^2}. \tag{1}$$

Under the action of a constant stretching force F applied to its ends and directed along the z axis (the ends are otherwise unconstrained and no torque is applied), the helix deforms into a curve whose shape is determined by minimizing the elastic energy [6–9]

$$E = \frac{1}{2}\sum_{i=1}^{3} a_i \int_0^L ds[\delta\omega_i(s)]^2 - FR_z, \tag{2}$$

with respect to the deviations $\delta\omega_i(s)$ of the generalized curvatures and torsions $\omega_i(s)$ from their spontaneous values in the undeformed state (s is the contour parameter). In general, these quantities are related to the (in principle, arc-length dependent) curvature κ, torsion τ, and the angle α between one of the principal axes of the cross section ($\mathbf{t}_1$) and the binormal: $\omega_1 = \kappa\cos\alpha$, $\omega_2 = \kappa\sin\alpha$, and $\omega_3 = \tau + d\alpha/ds$. We study here the case that the only contribution to spontaneous twist comes from torsion ($\alpha_0 = 0$) and therefore $\omega_{01} = \kappa_0$, $\omega_{02} = 0$, and $\omega_{03} = \tau_0$, where the subscript 0 refers to the quantities in the undeformed state, a helix characterized as in Eq. (1). The coefficients a_1 and a_2 are bending rigidities associated with the principal axes of inertia of the (in general, noncircular) cross section, and a_3 is the twist rigidity. In the following we treat a_i as given material parameters of the spring. The shape of the deformed spring can be

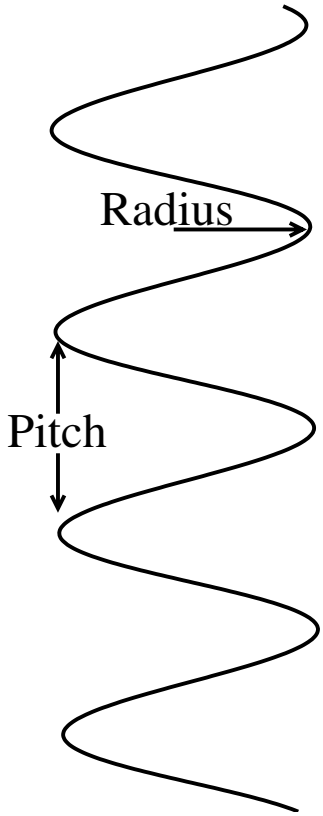

FIG. 1. A typical helix, with the pitch and radius indicated.

 0031-9007/03/90(2)/024301(4)$20.00

obtained by inserting the $\{\omega_i(s)\}$ that minimize the elastic energy into the generalized Frenet equations for the unit vectors $\mathbf{t}_i$ ($\mathbf{t}_3$ is the tangent to the curve at point s and $\mathbf{t}_1$ and $\mathbf{t}_2$ point along the principal axes of symmetry of the cross section):

$$d\mathbf{t}_i/ds = -\sum_{jk} e_{ijk}\omega_j\mathbf{t}_k, \tag{3}$$

where e_{ijk} is the antisymmetric unit tensor [10]. The space curve $\mathbf{r}(s)$ associated with the centerline of the deformed spring is then obtained by integrating the relation $d\mathbf{r}/ds = \mathbf{t}_3$. The system of equations is closed by substituting the expression for the projection of the end-to-end vector on the z axis, $R_z = \int_0^L ds\mathbf{t}_3(s)\cdot\mathbf{z}$, into Eq. (2). Since the spring will always orient itself along the direction of the force, in the following we replace R_z by the end-to-end distance R.

The force-extension curves are calculated numerically for a helix of four turns by finding a set of $\omega_i(s_j)$ (the continuous curve is replaced by a discrete set of points, $\{s_j\}$, $j = 1, 2, \ldots$), that minimizes the energy, Eq. (2). Two typical types of behavior are found. For sufficiently large ratio of pitch to radius $p/r = 2\pi\tau_0/\kappa_0$ and sufficiently small ratio of twist to bending rigidity a_3/a_b [where $a_b^{-1} = (a_1^{-1} + a_2^{-1})/2$], the deformation is continuous and identical curves are obtained by stretching the undeformed helix and by starting from a fully stretched configuration and decreasing the tensile force to zero (Fig. 2).

In the opposite limit (sufficiently large r/p and a_3/a_b ratios), increasing F results in a sequence of discontinuous upward jumps of the end-to-end distance (Fig. 3), whose number depends on the number of helical turns and on the increment of the force. Comparison of the conformations on both sides of a discontinuity shows that the jumps are associated with the elimination of helical turns (Fig. 3, insets). Discontinuous downward jumps of the end-to-end distance are also observed when one starts from a fully stretched configuration and gradually decreases the tensile force, but the locations of these jumps are, in general, different from those of the upward ones. The observation of hysteresis loops of stretching and contraction implies that the elastic energy $E(R)$ has multiple local minima whose depth and location vary with the tensile force F. In the absence of thermal fluctuations, and with infinitesimal force increments, a transition to a new energy minimum (not necessarily the lowest energy one) takes place when the minimum corresponding to the original state disappears. In practice, the size of the hysteresis loop is a function of the size of the force increments chosen.

There exists a critical surface in the parameter space that separates between regions in which the deformation is continuous from those in which a discontinuous stretching transition takes place. It is of particular interest to locate this critical surface in the limit of an infinitely long helix, for which end effects are negligible and it is expected that the only stable states are perturbations of the original undeformed helix and of the completely stretched spring (and therefore only one hysteresis loop that corresponds to a single stretching and a single contraction instabilities is expected). Insight into this limit can be achieved via analytical approximations. In order to reduce the number of variables, we consider a ribbon with highly asymmetric cross section, $a_2/a_1 \to \infty$, in which case the cross section of the ribbon is pinned to the Frenet frame of its centerline, $\alpha(s) = 0$, and the deformed spring is completely characterized by κ and τ. Based on our

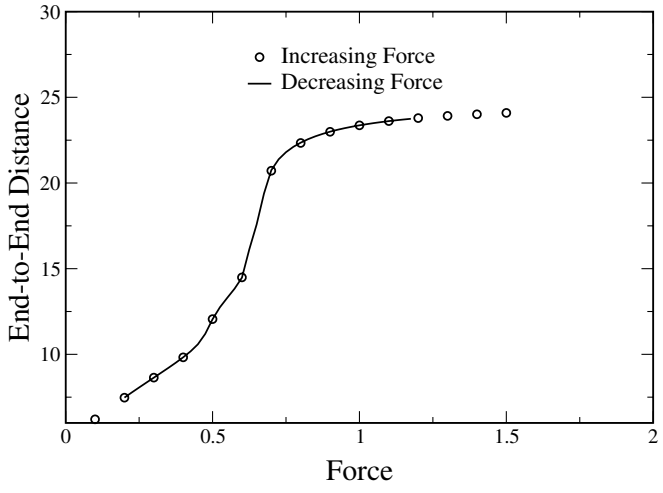

FIG. 2. Continuous deformation of a helix of four turns with $\kappa_0 = 1$, $\tau_0 = 0.2$, $a_1 = 1$, $a_2 = 5$, $a_3 = 3$, showing absence of hysteresis. We show the end-to-end distance as a function of the force for both increasing (circles) and decreasing (solid line) force.

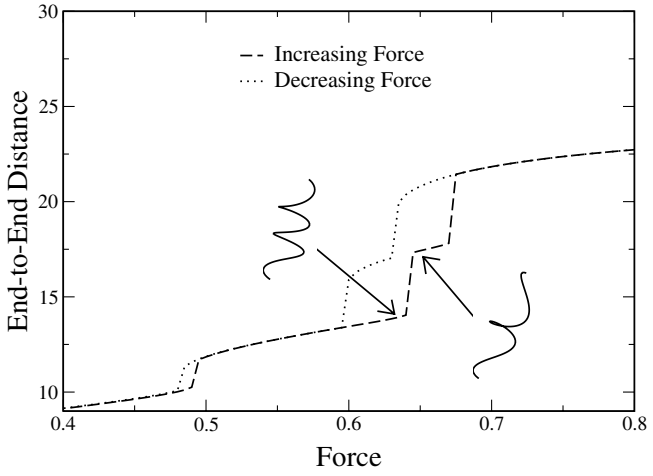

FIG. 3. Hysteresis loop for a helix of four turns, now with $a_3 = 4$. The other parameters are as in Fig. 2. We again show the end-to-end distance as a function of the force for both increasing and decreasing force.

numerical studies of short helices, we stress that varying a_2 (while keeping all other parameters fixed) affects the detailed extension versus force curves but does not change the character of the transitions, and stretching instabilities accompanied by hysteresis are observed even in the symmetric case, $a_1 = a_2$.

In the following we measure the energy in units of $a_1\kappa_0^2 L$, and force in units of $a_1\kappa_0^2$. In order to obtain analytical results, we consider the limit of an infinitely long helix and assume that the spring maintains a helical shape and responds to deformation only by adjusting its curvature and torsion parameters. Thus, we look for constant (s-independent) parameters κ and τ that minimize the energy per unit length,

$$E/L = \frac{1}{2}(\kappa/\kappa_0 - 1)^2 + \frac{a_3/a_1}{2}(\tau/\kappa_0 - \tau_0/\kappa_0)^2 - \frac{F\tau/\kappa_0}{\sqrt{(\kappa/\kappa_0)^2 + (\tau/\kappa_0)^2}}. \quad (4)$$

Support for this variational approximation comes from numerical minimization of the energy, Eq. (2), which shows that while the curvature and torsion oscillate about their mean values, the amplitude of oscillation decreases with the length of the spring. In Fig. 4 we compare the extension vs force curve for a helix of 12 turns, obtained by exact numerical minimization of Eq. (2), with that obtained using the variational estimate. The fact that the two curves coincide up to the stability limits of the initial and the final states provides further support for the validity of our variational approach. Beyond these limits, the deformed object is not close to a pure helix, and our simple estimates are inappropriate.

Analytical results can be obtained in several limiting cases. In the case of large twist rigidity, $a_3/a_1 \to \infty$, the torsion is pinned to its spontaneous value ($\tau = \tau_0$) and the curvature obeys the relation $a_1(\kappa/\kappa_0 - 1) + F(\tau_0/\kappa_0) \times (\kappa/\kappa_0)[(\kappa/\kappa_0)^2 + (\tau/\kappa_0)^2]^{-3/2} = 0$. Graphical analysis of this equation shows that it admits either a single minimum or two minima separated by a maximum. For $\tau_0 > \tau_{0,c}$ there is a single minimum of κ as a function of F. For $\tau_0 < \tau_{0,c}$, there is a window of F between which there are three solutions and outside which there is only one solution. This window closes at the critical point: $\tau_{0,c}/\kappa_0 = (2/3)^{5/3} = 0.363$, $F_c = 0.651$, and $\kappa_c/\kappa_0 = 0.444$. Another limit in which the critical point can be calculated analytically for arbitrary a_3/a_1 is $\tau_0/\kappa_0 \ll 1$. In this case we find that two minima exist for $a_3/a_1 > 4/3$. The critical value of this ratio is therefore $4/3$ and at this point $F_c = 4/3$, and $\kappa_c/\kappa_0 \simeq 54^{1/5}(\tau_0/\kappa_0)^{2/5}/2$. In between these two limits the critical points have to be found numerically, resulting in a critical line in the $a_3/a_1 - \tau_0/\kappa_0$ plane (Fig. 5). These analytic results are consistent overall with the general features seen in our numerical solutions for finite length helices. One striking difference is in the number of metastable states. The finite helix has many such metastable states, whereas the infinite helix has only two, the stretched and the unstretched. From the numerics it appears that as the number of turns increases, the number of states goes up, and the depth of the corresponding wells shrinks so as to leave only two metastable states in the limit of an infinite number of turns.

We have shown that there exists a range of spontaneous curvatures and torsions as well as bending and twist rigidities in which a helical spring does not deform continuously with the tensile force. Instead, as the force is increased, the spring undergoes a sequence of stretching instabilities. Hysteresis is predicted to take place when the force is decreased starting from full extension, as

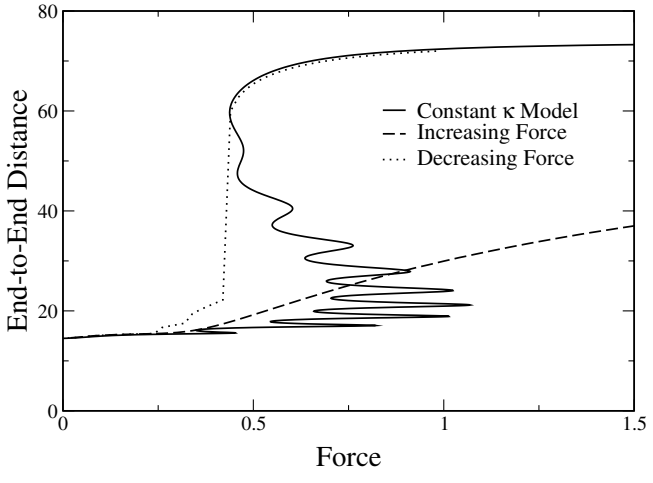

FIG. 4. Hysteresis loop for a helix of 12 turns, with $\kappa_0 = 1$, $\tau_0 = 0.2$, $a_1 = 1$, $a_2 = a_3 = \infty$. We show the end-to-end distance as a function of the force for both increasing (dashed line) and decreasing (dotted line) force. Also shown is the result of our simple model with constant κ (solid line).

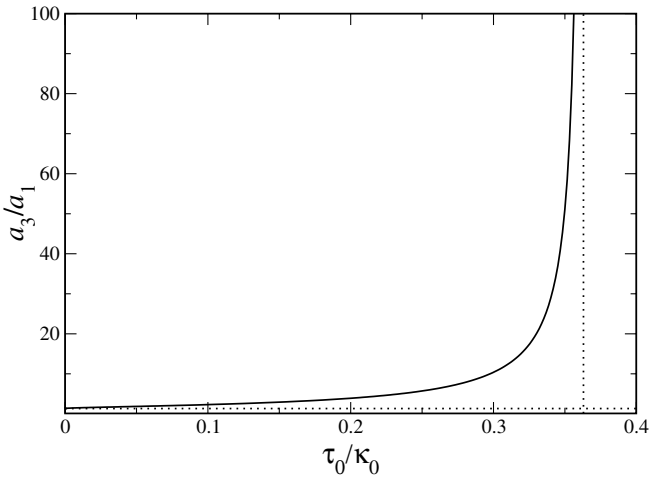

FIG. 5. Critical line in the $a_3/a_1 - \tau_0/\kappa_0$ plane for an infinitely long helix with $a_2/a_1 \to \infty$. The vertical and horizontal dotted lines correspond to the two limits discussed in the text, $\tau_{0,c}/\kappa_0 = 0.363$ and $a_3/a_1 = 1.333$, respectively.

both the number of sudden contractions and their locations differ from that of the stretching instabilities at increasing force. We presented a variational calculation of the critical line that separates the region of parameters in which the deformation varies continuously with the force from that in which stretching instabilities take place. Even though the analysis was restricted to the limit of an infinitely long spring with a highly asymmetric cross section, our numerical results indicate that stretching instabilities will be observed in helical springs with both the radius to pitch ratio and the ratio of twist rigidity to bending rigidity larger than some numbers of order unity. While the former requirement can be realized by preparing a spring of a desired shape, the latter condition may require the use of materials with special elastic properties. Notice that for isotropic materials the rigidities can be expressed in terms of the shear and Young moduli μ and E and the geometry of the cross section; for example, in the case of a rectangular cross section with sides c_1 and c_2 one has [11] $a_1 = Ec_1c_2^3/12$, $a_2 = Ec_1^3c_2/12$, and $a_3 \simeq \mu c_1c_2^3/3$ (the last expression holds in the limit $c_1 \gg c_2$). For incompressible materials this yields $a_3/a_1 \simeq 4/3$ which coincides with the critical value of the ratio. The ratio a_3/a_1 can be increased beyond this critical value by reducing the Poisson ratio or by using anisotropic materials with high resistance to twist.

We close with some final comments about the generality and applicability of our findings. First, we point out that insofar as our instability is critically dependent of the geometry of the helix (namely, the pitch/radius ratio), it has no obvious relation to the Euler buckling instability of beams. However, like the Euler instability, the instability discussed here is a result of the simplest theory of continuum elasticity of slender rods, and should be present independent of any fine details of the underlying microscopic structure. The geometry dependence of the effect is noteworthy; it exists only for low-pitch helices, and not for rodlike ones. In fact, the limit of a straight rod is trivial in our model as it is inextensible—the "stretchiness" of the helix is a consequence of its low pitch.

Finally, we stress that since the present analysis is purely mechanical [12], the results are directly applicable only to macroscopic objects. The relevance of the present work to the deformation of nano-objects such as biopolymers (DNA, proteins), protein filaments (actin, microtubules, etc.), and carbon nanotubes depends on the question of whether these objects possess spontaneous curvature and torsion, and on the values of the bending rigidities. It is interesting to note that in elastic models of DNA [13] a_3 is commonly assumed to exceed a_1, as is required for our effect. A stretching instability has in fact been recently observed in self-assembled helical ribbons of cholesterol [3]. Whether this observation is related to our theory remains to be explored. Furthermore, both hysteresis and a sequence of stretching instabilities were reported for chromatin (a zigzag of nucleosomes connected by linker DNA) [4]. Discontinuous stretching transitions were also reported in single molecule extension studies of torsionally constrained DNA at high degree of supercoiling(unlike our model, supercoiling was not spontaneous but was achieved by the application of torque) [5]. The study of stretching instabilities of such objects requires consideration of thermal fluctuations and extension of the present analysis using the methods of references [9,10,14,15], which we hope to report on soon.

D. A. K. and Y. R. acknowledge the support of the Israel Science Foundation.

[1] A. E. H. Love, *A Treatise on the Mathematical Theory of Elasticity* (Dover, New York, 1944).
[2] S. P. Timoshenko and J. M. Gere, *Theory of Elastic Stability* (McGraw-Hill, New York, 1963).
[3] B. Smith, Y.V. Zastavker, and G. B. Benedek, Phys. Rev. Lett. **87**, 278101 (2001).
[4] Y. Cui and C. Bustamente, Proc. Natl. Acad. Sci. U.S.A. **97**, 127 (2000).
[5] T. R. Strick, J.-F. Allemand, D. Bensimon, A. Bensimon, and V. Croquette, Science **271**, 1835 (1996).
[6] Lord Kelvin and P. G. Tait, *Treatise on Natural Philosophy* (University Press, Cambridge, 1883).
[7] P. Nelson, Phys. Rev. Lett. **80**, 5810 (1998).
[8] R. E. Goldstein, A. Goriely, G. Huber, and C.W. Wolgemuth, Phys. Rev. Lett. **84**, 1631 (2000).
[9] S. Panyukov and Y. Rabin, Europhys. Lett. **57**, 512 (2002).
[10] S. Panyukov and Y. Rabin, Phys. Rev. Lett. **85**, 2404 (2000); Phys. Rev. E **62**, 7135 (2000).
[11] L. D. Landau and E. M. Lifshitz, *Theory of Elasticity* (Pergamon Press, Oxford, 1986).
[12] For different types of bifurcations that appear in supercoiled elastic rings, see B. D. Coleman, D. Swigon, and I. Tobias, Phys. Rev. E **61**, 759 (2000).
[13] J. Shimada and H. Yamakawa, Macromolecules **17**, 689 (1984).
[14] Y. Kats, D. A. Kessler, and Y. Rabin, Phys. Rev. E **65**, 020801 (2002).
[15] D. A. Kessler and Y. Rabin, J. Chem. Phys. **118**, 897 (2002).